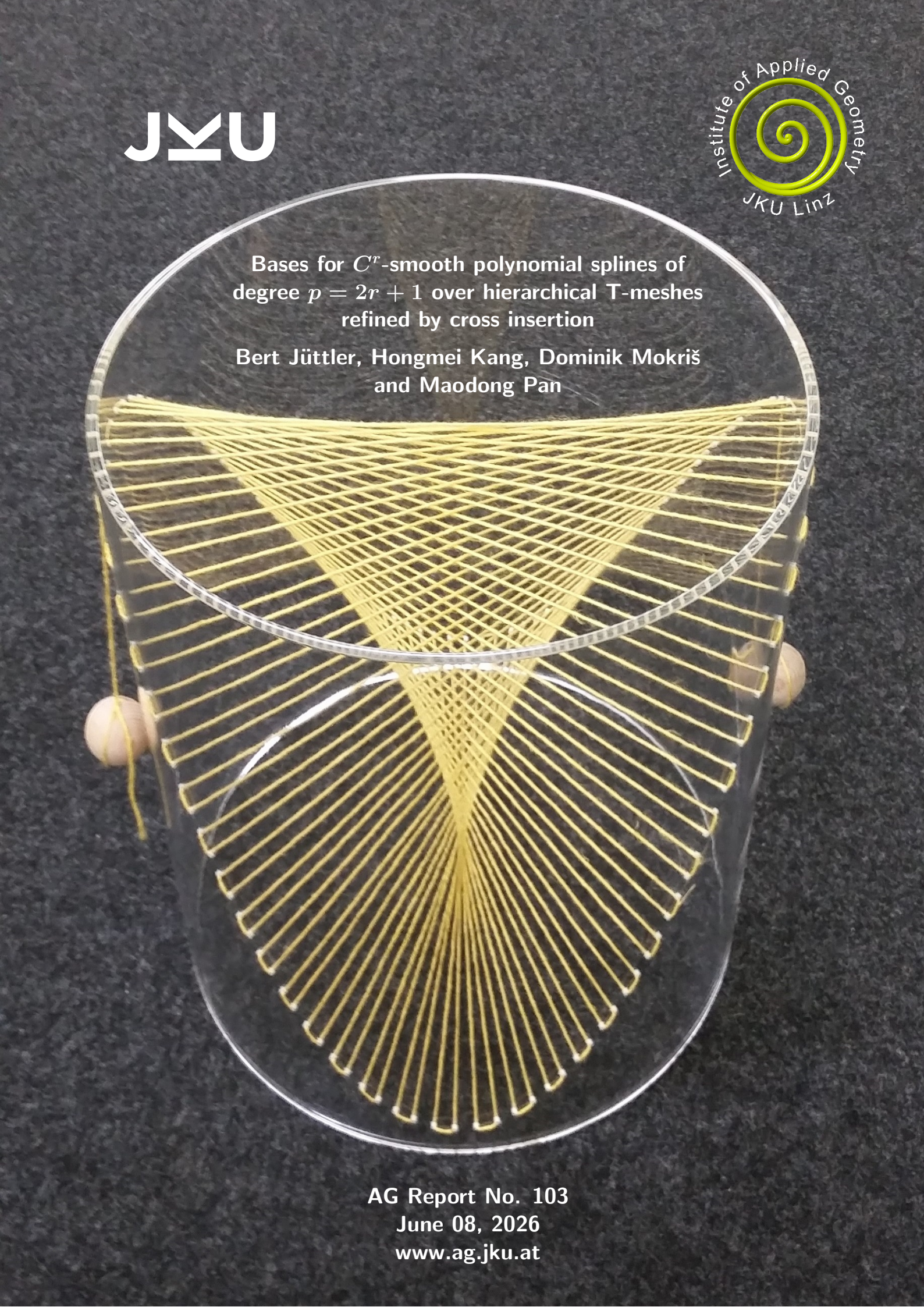

Bases for C^r-smooth polynomial splines of degree $p = 2r + 1$ over hierarchical T-meshes refined by cross insertion

Bert Jüttler, Hongmei Kang, Dominik Mokriš and Maodong Pan

AG Report No. 103
June 08, 2026
www.ag.jku.at

Bases for C^r-smooth polynomial splines of degree $p = 2r + 1$ over hierarchical T-meshes refined by cross insertion

Bert Jüttler, Hongmei Kang, Dominik Mokriš and Maodong Pan

Abstract This paper compares the various bases for C^r-smooth polynomial splines of degree $p = 2r + 1$ over hierarchical T-meshes refined by cross insertion. This class of splines is fundamental for geometric design and isogeometric analysis, as it provides a framework for local refinement that overcomes the limitations of traditional NURBS. We provide a systematic overview and comparative analysis of five constructions: PHT-splines, HB-splines, THB-splines, MPHT-splines and NPHT-splines. Our theoretical analysis examines key properties including (local) linear independence, completeness, partition of unity, support characteristics and the proportion of tensor-product B-splines present in the basis. It indicates that MPHT-splines emerge as a particularly advantageous option, since they preserve all desirable properties of PHT-splines and THB-splines while possessing a higher proportion of tensor-product B-splines. Additionally, we establish a link between NPHT-splines and another adaptive spline construction, as well as the local linear independence property of PHT-, THB-, and MPHT-splines.

1 Introduction

Tensor product splines form the mathematical backbone of computer aided geometric design and have been successfully adopted as the underlying mathematical

Bert Jüttler
Johannes Kepler University, Linz, Austria, e-mail: bert.juettler@jku.at

Hongmei Kang
Soochow University, Suzhou, China, e-mail: khm@suda.edu.cn

Dominik Mokriš
MTU Aero Engines, München, Germany, e-mail: dominik.mokris@mtu.de

Maodong Pan
Nanjing University of Aeronautics and Astronautics, China, e-mail: mdpan@mail.ustc.edu.cn

technology for isogeometric analysis. Their structured, regular topology provides a powerful and computationally efficient framework that elegantly unifies geometric representation and numerical simulation within a single language. Despite their advantages, the global structure of tensor product splines has an inherent limitation: Any local refinement operation is propagated throughout the entire parameter domain. This leads to significant computational inefficiency when dealing with problems exhibiting localized phenomena. For this reason, developing locally refinable splines that break the rigid tensor product topology has become a major area of research. Examples of these developments include HB-splines [16], T-splines [29], PHT-splines [4], THB-splines [8] and LR B-splines [5].

Hierarchical B-splines (HB-splines) [16] overcome the drawback of NURBS by constructing a basis through a sequence of nested B-spline spaces. This is achieved by organizing different resolution levels in a hierarchical manner. While HB-splines inherit most properties of NURBS such as non-negativity, local support and linear independence, they do not form a partition of unity. This directly motivated the development of truncated hierarchical B-splines (THB-splines) [8], which were designed specifically to overcome this limitation. Additionally, THB-splines have advantages regarding the numerical properties of the resulting discretizations [7], and their coefficient-preserving properties facilitate the effortless construction of spline projectors [31].

T-splines [29] are another generalization of standard NURBS. Their primary innovation is the introduction of T-junctions within the control grid. Unlike NURBS, which require a tensor-product grid of control points, T-splines allow for rows of control points to terminate locally, creating a T-shaped connection. This "T-junction" capability makes the control mesh much more flexible and efficient. While standard T-splines offer superior geometric flexibility for modeling, their arbitrary T-junction configurations can sometimes lead to linear dependency in the resulting set of blending functions, which poses significant challenges for numerical simulation. Analysis-suitable T-splines (AST-splines) [17] were developed explicitly to ensure linear independence. These splines impose certain constraints on the distribution of the T-joints.

PHT-splines [4], with the acronym standing for "Polynomial Splines over Hierarchical T-meshes", enable selective local mesh refinement through their characteristical hierarchical T-mesh structure. The construction begins with a coarse tensor-product mesh and progressively refines specific cells through cross insertions. This results in a hierarchical structure with T-junctions. Through the use of function truncation and reconstruction, PHT-splines maintain linear independence, local support, and partition of unity properties while avoiding the computational overhead of global refinement.

The so-called "locally refined" (LR) B-splines [5] were designed to explicitly provide highly flexible local refinement, thereby ensuring the nestedness of the resulting spaces. Once more, the construction begins with a coarse tensor-product mesh in the parameter domain. This mesh is refined by inserting line segments vertically or horizontally.

Unlike the hierarchical structure of PHT- or (T)HB-splines, LR B-splines maintain a single-level system of B-spline blending functions. However, LR B-splines do not inherit some important properties from traditional NURBS, such as linear independence and partition of unity. Subsequently, several specific mechanisms [1, 26, 27, 28] embedded within the framework of LR B-splines were proposed to ensure that the basis functions remain linearly independent.

The development of HB-splines, T-splines, PHT-splines and LR B-splines has significantly advanced the fields of geometric design and isogeometric simulations. So far, they have been successfully used for domain parameterizations [6, 2, 21, 35], surface fitting [13, 14, 32] and topology optimization [11, 20, 33, 34], among many other applications.

On the theoretical side, a central issue is the question of *algebraic completeness*: given a mesh and a spline construction scheme, does it span the full space of spline functions of a specified degree and smoothness on the mesh? This problem of algebraic completeness for spline spaces has been studied in the context of hierarchical splines [19], and is naturally satisfied by PHT-splines according to their dimension properties. The completeness property is not only of theoretical interest but also essential for constructing isogeometric discretizations based on de Rham complexes [30].

Regarding computational efficiency, it has been observed that the presence of a tensor-product structure – even if only locally – significantly facilitates the isogeometric matrix assembly process [18, 22, 23, 24]. For instance, using HB-splines in assembly can be more efficient than using THB-splines.

The purpose of this paper is to provide a systematic overview and comparative analysis of different constructions for PHT-spline spaces. We aim to clarify their similarities and differences, with particular emphasis on evaluating their potential to preserve tensor-product structures – a feature crucial for both theoretical completeness and efficient numerical simulations.

The remainder of the paper is structured as follows. We begin by introducing the fundamental spline space in Section 2, which defines hierarchical T-meshes and reviews the dimension theorem for C^r-smooth polynomial splines. Section 3 covers the essential concepts of tensor-product B-splines and B-systems, and defines the truncation operator along with its key properties. The core of the paper is devoted to presenting four kinds of hierarchical spline constructions. We first detail PHT-splines in Section 4, describing their selection criterion and truncation algorithm. This is followed by an explanation of HB- and THB-splines in Section 5, which employ a support-based selection criterion. Subsequently, we introduce modified PHT-splines in Section 6, a variant that replaces truncated functions with tensor-product splines for rectangular supports. Finally, we present the New PHT-splines in Section 7, which are constructed by using an additional tensorization step. We also link them to the LR B-splines. To compare the different approaches, Section 8 provides a theoretical analysis of all four spline types, examining their properties including completeness, linear independence, local linear independence, partition of unity, support characteristics, and tensor-product structure. The paper concludes in Section 9 with directions for future work.

2 The spline space

We recall the definition of the space of C^r-smooth polynomial splines of degree $p = 2r + 1$ over hierarchical T-meshes that are refined solely by cross insertion. More precisely, the construction starts with a regular initial mesh consisting of level 0 cells. Higher-level cells are subsequently created by splitting the previous level's cells.

To guide the refinement process, we assume that two (one for each coordinate direction) bi-infinite, strictly monotonic node sequences

$$\xi_i^\ell, \quad \eta_j^\ell, \quad i, j \in \mathbb{Z},$$

are given for each level $\ell = 0, 1, 2, \ldots, L$. The nodes must fulfill the dyadicity equations

$$\xi_{2i}^{\ell+1} = \xi_i^\ell, \quad \eta_{2j}^{\ell+1} = \eta_j^\ell \, .$$

For each level ℓ, the node sequences define a *rectangular grid*

$$\Gamma^\ell = \{\{\xi_i^\ell\} \times \mathbb{R} | \; i \in \mathbb{Z}\} \cup \{\mathbb{R} \times \{\eta_j^\ell\} : \; j \in \mathbb{Z}\}$$

and a set of *vertices*

$$V^\ell = \{(\xi_i^\ell, \eta_j^\ell) \mid i, j \in \mathbb{Z}\} \, .$$

Each rectangular grid is contained within the grid of the previous level, and each vertex is also a vertex of all higher-level grids. However, we always use the lowest possible level when referring to the *level of a vertex.*

The connected components of $\mathbb{R}^2 \setminus \Gamma^\ell$ are the *cells* of level ℓ, which we collect into sets Z^ℓ. Uniform grids are obtained by selecting uniform node sequences $\xi_i^\ell = \eta_i^\ell = 2^{-\ell} i$ at every level.

In addition to these grids and vertices, we consider a sequence of nested domains (i.e., bounded open subsets of $\mathbb{R}^2$)

$$\Omega^0 \supseteq \Omega^1 \supseteq \Omega^2 \supseteq \cdots \supseteq \Omega^L \, .$$

The boundary of each domain of level $\ell \geq 1$ is required to be a subset of the grid of the preceding level,

$$\partial\Omega^\ell \subset \Gamma^{\ell-1} \, .$$

Equivalently, each domain is required to be a union of a certain set of cells from the previous level.

The boundary of the initial domain is contained in the coarsest grid, $\partial\Omega^0 \subset \Gamma^0$, and is closed and simple. More generally, it could even be a union of mutually disjoint simple polygons, but then the resulting connected components could be analyzed and dealt with separately.

We will refer to these domains as *subdomains* since they are all contained within the lowest-level domain Ω^0. The latter serves as the domain of the spline functions considered in this paper.

For later reference we introduce the *partially closed subdomains*

$$\widehat{\Omega^\ell} = \overline{\Omega^\ell} \setminus (\partial\Omega^\ell \cap \Omega^0) ,$$

which are obtained by including all the boundary points that are located on the boundary of Ω^0. In particular, we get $\widehat{\Omega^0} = \overline{\Omega^0}$.

The *hierarchical T-mesh*

$$M = \bigcup_{\ell=0}^{L} \{c \in Z^\ell \mid \Omega^\ell \supseteq c \not\subseteq \Omega^{\ell+1}\}$$

is the selection of the cells of all the levels that are simultaneously active (contained in the subdomain of the same level) and unrefined (not contained in subdomains of higher levels). Note that we define $\Omega^{L+1} = \emptyset$ for simplicity. The difference set

$$\mathcal{G} = \overline{\Omega^0} \setminus M$$

is called the *hierarchical grid*.

We denote with

$$\mathcal{P}^{2r+1} = \langle 1, x, \ldots, x^{2r+1}, y, xy, \ldots, x^{2r+1}y, \ldots, y^{2r+1}, xy^{2r+1}, \ldots, x^{2r+1}y^{2r+1} \rangle$$

the space of the tensor-product bivariate polynomials of degree $2r + 1$. The *spline space*

$$\mathcal{S} = \{s \in C^r(\Omega^0) \mid \forall c \in M \ : \ s|_c \in \mathcal{P}^{2r+1}\},$$

consists of all C^r-smooth functions that can be obtained by piecing together polynomial segments over the cells of the mesh. The dimension of the space has been established in the literature:

Theorem 1 (Deng et al. [3]) *The spline space $\mathcal{S}$ has the dimension $n(r+1)^2$, where n is the total number of cross and boundary vertices of the hierarchical grid $\mathcal{G}$. Each spline function s is uniquely determined by prescribing the values and derivatives*

$$\frac{\partial^p}{\partial x^p}\frac{\partial^q}{\partial x^q} s(x, y), \quad p, q = 0, \ldots, r , \tag{1}$$

at each cross or boundary vertex.

3 Tensor-product B-splines and truncation

Recall that *B-splines* are piecewise polynomial functions of a given degree that are derived from knot sequences. The symbol $N_\Xi^{2r+1}(x)$ – and similarly $N_H^{2r+1}(y)$ – represents the B-spline of degree $2r + 1$ with the variable x that is defined by the $2r + 3$ knots contained in the local knot sequence denoted by Ξ. The products

$$N_{\Xi}^{2r+1}(x) N_{\mathrm{H}}^{2r+1}(y)$$

are the *tensor-product B-splines*. For any pair of monotonically increasing node triplets (ξ', ξ'', ξ''') and (η', η'', η'''), we define a set

$$B_{(\xi', \xi'', \xi'''), (\eta', \eta'', \eta''')} \tag{2}$$

of tensor-product B-splines called the *B-system* defined by these triplets. The system consists of the $(r+1)^2$ tensor-product B-splines

$$N_{\Xi_p}^{2r+1}(x) N_{\mathrm{H}_q}^{2r+1}(y) \ , \ p, q = 0, \ldots, r \ ,$$

defined by the knot sequences

$$\begin{aligned} \Xi_p &= (\underbrace{\xi', \ldots, \xi'}_{r+1-p \text{ times}}, \underbrace{\xi'', \ldots, \xi''}_{r+1 \text{ times}}, \underbrace{\xi''', \ldots, \xi'''}_{p+1 \text{ times}}) \quad \text{and} \\ \mathrm{H}_q &= (\underbrace{\eta', \ldots, \eta'}_{r+1-q \text{ times}}, \underbrace{\eta'', \ldots, \eta''}_{r+1 \text{ times}}, \underbrace{\eta''', \ldots, \eta'''}_{q+1 \text{ times}}) \ . \end{aligned}$$

In particular, we will use the B-systems defined by adjacent nodes at the same level,

$$B_{ij}^{\ell} = B_{(\xi_{i-1}^{\ell}, \xi_i^{\ell}, \xi_{i+1}^{\ell}), (\eta_{j-1}^{\ell}, \eta_j^{\ell}, \eta_{j+1}^{\ell})} \ ,$$

these are the *B-systems of level ℓ associated with the vertex* $(\xi_i^{\ell}, \eta_j^{\ell})$. The union of these B-systems

$$\mathbb{F}^{\ell} = \bigcup_{i,j \in \mathbb{Z}} B_{i,j}^{\ell} \ . \tag{3}$$

is the *basis of the full space of tensor-product splines of level ℓ*. Any linear combination

$$f(x, y) = \sum_{\beta \in \mathbb{F}^{\ell}} c_{\beta} \, \beta(x, y) \tag{4}$$

with real coefficients c_{β} is a *tensor-product spline function* of level ℓ. Such a spline function possesses representations with respect to the B-systems of higher levels, hence it is simultaneously a tensor-product spline function of any level $k \geq \ell$.

In the representation (4), the coefficients of the B-splines associated with a vertex $(\xi_i^{\ell}, \eta_j^{\ell})$ are uniquely determined by prescribing the values and the partial derivatives

$$\frac{\partial^p}{\partial x^p} \frac{\partial^q}{\partial x^q} f(\xi_i^{\ell}, \eta_j^{\ell}) \tag{5}$$

of order not exceeding r with respect to x and y (which are considered separately) at that vertex, i.e., for indices $p, q = 0, \ldots, r$. Among the B-systems considered in (3), exactly those associated with a vertex $(\xi_i^{\ell}, \eta_j^{\ell})$ have non-zero values and derivatives listed in (5) at that vertex.

Let the set $R \subset \mathbb{F}^\ell$ be a collection of some B-systems of level ℓ. Given a spline function f of level ℓ, we *truncate* it with respect to the set of B-splines $\bigcup R$ in this collection by assigning zero values to all the spline coefficients c_β associated to tensor-product B-splines in R. More precisely, we define the *truncation with respect to the set R* as

$$(\mathrm{trc}_R^\ell f)(x,y) = \sum_{\beta \in \mathbb{F}^\ell \setminus \bigcup R} c_\beta \beta(x,y) \ .$$

For future reference we note a property of the truncation operator:

Lemma 2 *The values and derivatives of the truncated function considered in* (1) *are equal to zero at all vertices associated with B-systems in the set R.*

Proof This is implied by the fact that among the B-splines in the set $\mathbb{F}^\ell$, only those associated with a vertex $(\xi_i^\ell, \eta_j^\ell)$ take non-zero values at that vertex. □

For ease of notation, we generalize the truncation operator to *sets of spline functions* by applying it to each of the spline functions individually. When applied to a set F of spline functions, the result

$$\mathrm{trc}_R^\ell F = \{\mathrm{trc}_R^\ell f \mid f \in F\}$$

is again a set of spline functions. Furthermore, we generalize the truncation operator to *sets of sets of spline functions* by performing the truncation for each set of spline functions individually. When applied to a set S of sets of spline functions, the result

$$\mathrm{trc}_R^\ell S = \{\mathrm{trc}_R^\ell F \mid F \in S\}$$

is again a set of sets of spline functions.

4 PHT-splines

The PHT-splines, which were introduced by Deng et al. [4], form a basis of the spline space $\mathcal{S}$. They are generated by the construction described below:

Step 1. First we *select* active tensor-product B-splines from all levels. More precisely, one B-system is selected for each cross vertex and each vertex on the subdomain boundary $\partial\Omega^0$, using the level of each vertex. For each level ℓ, the selected B-systems are gathered in a set of B-systems

$$S_{\mathrm{PHT}}^\ell = \{B_{i,j}^\ell \mid (i,j) \in \mathcal{I}_{\mathrm{PHT}}^\ell\} \ ,$$

which is defined with the help of the index set

$$\mathcal{I}_{\mathrm{PHT}}^\ell = \{(i,j) \in \mathbb{Z}^2 \mid (\xi_i^\ell, \eta_j^\ell) \in \widehat{\Omega^\ell} \setminus V^{\ell-1}\} \ .$$

In particular, considering the coarsest level we have

$$\mathcal{I}^0_{\mathrm{PHT}} = \{(i,j) \in \mathbb{Z}^2 \mid (\xi^0_i, \eta^0_j) \in \widehat{\Omega^0}\}$$

since we define $V^{-1} = \emptyset$. Each S^ℓ_{PHT} for $\ell = 0, \dots, L$ is a set of sets of B-splines.

Step 2. Second, we iteratively *truncate and enrich* these sets of B-systems. We initialize the construction with the B-systems selected at the coarsest level. Then, we iteratively *truncate* the functions with respect to the selected B-systems of the next level. Simultaneously, we *enrich* the basis by adding the very systems.

More precisely, we define

$$T^\ell_{\mathrm{PHT}} = (\mathrm{trc}^\ell_{\mathrm{PHT}}\, T^{\ell-1}_{\mathrm{PHT}}) \cup S^\ell_{\mathrm{PHT}}\,, \quad \ell = 0, \dots, N\,,$$

where we perform the truncation

$$\mathrm{trc}^\ell_{\mathrm{PHT}} = \mathrm{trc}^\ell_{S^\ell_{\mathrm{PHT}}}$$

with respect to all the B-splines in the systems that have been gathered in S^ℓ_{PHT}. This includes the initialization $T^0_{\mathrm{PHT}} = S^0_{\mathrm{PHT}}$ if one adopts the convention that $T^{-1}_{\mathrm{PHT}} = \emptyset$.

The resulting truncated and enriched sets of B-systems

$$T^\ell_{\mathrm{PHT}} = \bigcup_{k=0}^{\ell} \{B^{k,\ell}_{i,j} \mid (i,j) \in \mathcal{I}^\ell_{\mathrm{PHT}}\}$$

are formed by sets of selected B-systems of levels $k = 0, \dots, \ell$, which have been truncated $\ell - k$ times, i.e.,

$$B^{k,\ell}_{i,j} = \begin{cases} \mathrm{trc}^\ell_{\mathrm{PHT}}\, B^{k,\ell-1}_{i,j} & \text{if } k < \ell\,, \\ B^\ell_{i,j} & \text{if } k = \ell\,. \end{cases}$$

Each T^ℓ_{PHT} for $\ell = 0, \dots, L$ is a set of sets of B-splines.

Step 3. Finally we define the basis $\mathbb{B}_{\mathrm{PHT}} = \bigcup T^L_{\mathrm{PHT}}$.

This construction ensures the following property of the PHT-spline basis:

Corollary 3 *Only PHT-splines originating from exactly one of the B-systems (and subsequently truncated) take non-zero values and derivatives considered in* (1) *at each cross vertex and at each boundary vertex.*

Proof The proof of this fact is implied by Lemma 2. □

As a consequence, the PHT-splines form a *non-negative partition of unity*. The partition of unity property can be proved by constructing a spline function that interpolates the values (1) of the constant function $s = 1$. The non-negativity property is implied by the fact that truncation does not create negative spline coefficients.

Remark 4 The original construction of PHT splines is limited to rectangular domains Ω^0 and it uses $(2r+2)$-fold knots along the boundary, while inner knots are distributed

uniformly and have multiplicity $r + 1$. Here we present it for more general domains and non-uniform knots, and this is enabled by using B-splines with $(r + 1)$-fold knots, the values of which are taken from the two sequences of nodes.

Figure 1 depicts the B-systems formed by the PHT- and MPHT-splines (see Section 6) for a specific two-level hierarchical grid.

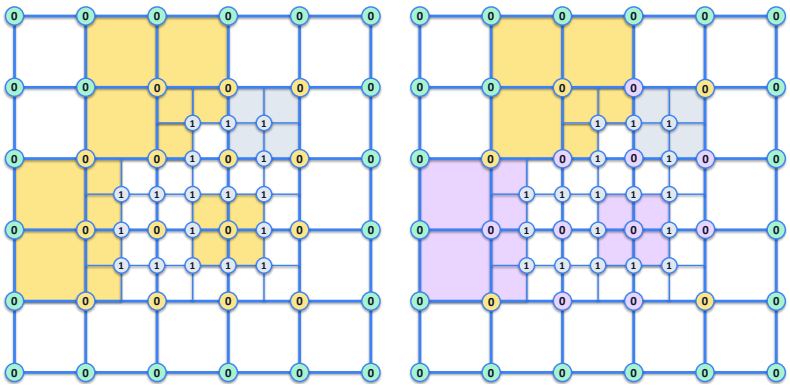

Fig. 1 B-systems formed by PHT- (left) and MPHT-splines (right) on a two-level hierarchical grid. For PHT-splines, the truncation reduces the support of the level-0 B-systems. Three level-0 instances and one level-1 instance are indicated in yellow and grey, respectively. For MPHT-splines, some of the truncated level-0 PHT-systems are modified into standard B-systems (purple).

5 HB- and THB-splines

The HB- and THB-splines were introduced by Kraft [16] and by Giannelli et al. [8], respectively. Considering them in the special case of tensor-product splines of degree $2r + 1$ with $(r + 1)$-fold knots, they form two bases of the spline space $\mathcal{S}$. These bases are generated by the constructions described below:

Step 1. First we *select* active B-systems from all levels. More precisely, we select B-systems of level ℓ whose support (which is restricted to its intersection with the largest domain Ω^0) is contained in the associated subdomain Ω^ℓ but not in the subdomain of the next higher level. In other words, when identifying a subdomain for further refinement, we eliminate the B-systems that can be represented as a linear combination of selected B-systems at finer levels. We obtain the sets of B-systems

$$S^\ell_{\mathrm{HB}} = \{B^\ell_{i,j} \mid (i,j) \in \mathcal{I}^\ell_{\mathrm{HB}}\} ,$$

which are defined with the help of the index sets

$$\mathcal{I}^\ell_{\mathrm{HB}} = \{(i,j) \in \mathbb{Z}^2 \mid \Omega^\ell \supseteq \operatorname{supp} B^\ell_{i,j} \not\subseteq \Omega^{\ell+1}\} .$$

In particular, considering the finest level we have

$$\mathcal{I}_{\mathrm{HB}}^{L} = \{(i,j) \in \mathbb{Z}^2 \mid \Omega^L \supseteq \operatorname{supp} B_{i,j}^{L}\} \ .$$

since we define $\Omega^{L+1} = \emptyset$. Note that we adopt the set-theoretical support definition,

$$\operatorname{supp} f = \{x \in \Omega^0 \mid f(x) \neq 0\} \ .$$

Each S_{HB}^{ℓ} for $\ell = 0, \ldots, L$ is a set of sets of B-splines.

Step 2. The HB-spline basis is obtained by forming the union of the sets of selected B-systems, $\mathbb{B}_{\mathrm{HB}} = \bigcup_{\ell=0}^{L} \mathcal{S}^{\ell}$.

Step 3. Second, we modify the HB-splines by iteratively *truncating* them,

$$T_{\mathrm{THB}}^{\ell} = (\mathrm{trc}_{\mathrm{THB}}^{\ell}\, T_{\mathrm{THB}}^{\ell-1}) \cup S_{\mathrm{HB}}^{\ell}$$

where we perform the truncation

$$\mathrm{trc}_{\mathrm{THB}}^{\ell} = \mathrm{trc}_{S_{\mathrm{THB}}^{\ell}}^{\ell} \ .$$

with respect to all the B-splines in the systems that have been gathered in S_{THB}^{ℓ}. We include the initialization $T_{\mathrm{THB}}^{0} = S_{\mathrm{HB}}^{0}$ by adopting the convention that $T_{\mathrm{THB}}^{-1} = \emptyset$.

Similarly to the case of the PHT-spline basis, which uses different index sets, the resulting truncated and enriched sets of B-systems

$$T_{\mathrm{THB}}^{\ell} = \bigcup_{k=0}^{\ell} \{B_{i,j}^{k,\ell} \mid (i,j) \in \mathcal{I}_{\mathrm{HB}}^{\ell}\}$$

are formed by sets of selected B-systems of levels $k = 0, \ldots, \ell$, which have been truncated $\ell - k$ times, i.e.,

$$B_{i,j}^{k,\ell} = \begin{cases} \mathrm{trc}_{\mathrm{THB}}^{\ell}\, B_{i,j}^{k,\ell-1} & \text{if } k < \ell \ , \\ B_{i,j}^{\ell} & \text{if } k = \ell \ . \end{cases}$$

Each T_{THB}^{ℓ} for $\ell = 0, \ldots, L$ is a set of sets of B-splines.

Step 4. Finally we define the basis $\mathbb{B}_{\mathrm{THB}} = \bigcup T_{\mathrm{THB}}^{L}$.

The construction of the THB-splines again ensures the following property, the proof of which is analogous to that of the PHT-spline basis:

Corollary 5 *Only THB-splines originating from exactly one of the B-systems (and subsequently truncated) take non-zero values and derivatives considered in* (1) *at each cross vertex and at each boundary vertex.*

As with PHT-splines, the THB-splines form a *non-negative partition of unity* as a consequence of this fact. The corollary does not apply to the HB-splines, however, and these splines do not sum to 1 in general.

Despite the different constructions, there is a striking similarity between the two bases:

Proposition 6 *The supports of the PHT- and THB-splines associated with the same cross or boundary vertex of the hierarchical mesh are identical.*

Proof We construct the B-systems of PHT- and THB-splines using an iterative procedure. We start with level 0 and refine the grid one level at a time. Consider the two B-systems, which are associated with a vertex $(\xi_i^\ell, \eta_j^\ell)$ of level ℓ. The PHT- and THB-splines are identical when the vertex is created, i.e., when refining the cells of level $\ell - 1$ in the subdomain Ω^ℓ. The two systems remain the same in all subsequent steps unless the vertex is located in $\widehat{\Omega}^\ell$. In this case, at level $\ell + 1$, the B-system of the THB-splines is replaced by a standard B-system of level $\ell + 1$, while the B-system of the PHT-splines is truncated. However, the result of the truncation is just a linear combination of the standard B-system of level $\ell + 1$, and thus has an identical support. Subsequent refinement steps may decrease the support further, but they do so identically for THB- and PHT-splines. □

The HB-splines have larger supports. They inherit the ordering of their associated vertices in the sense that only HB-splines of level ℓ or lower take non-zero values and derivatives considered in (1) at a level ℓ cross or boundary vertex of the hierarchical mesh. Based on this observation, the linear independence of HB-splines can be easily established.

Figure 2 depicts the B-systems formed by the HB- and THB-splines for a specific two-level hierarchical grid.

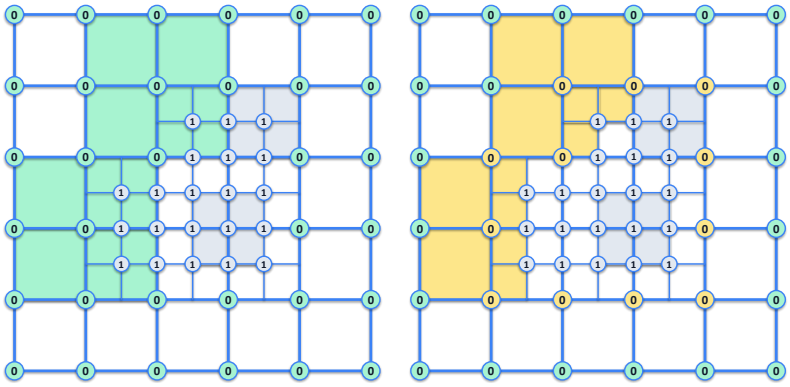

Fig. 2 B-systems formed by HB- (left) and THB-splines (right) on a two-level hierarchical grid. For HB-splines, the B-system supports are formed by two cells of the same level. Two supports are indicated for each level $\ell \in \{0, 1\}$ in green and grey, respectively. For THB-splines, the B-system supports are reduced due to truncation. The supports of two truncated level-0 systems and of two level-1 systems are indicated in yellow and grey, respectively.

6 Modified PHT-splines

Zhu and Chen [36] noted that the original construction of PHT-splines leads to numerical difficulties, due to the presence of multiple knots near the boundary.

Example: Decay phenomenon of univariate PHT-splines

In order to explain this phenomenon, we present univariate PHT-splines for $r = 1$ on the interval $\Omega^0 = (0, 2)$, which is globally refined twice, i.e., $\Omega^0 = \Omega^1 = \Omega^2$, see Fig. 3. The nodes of level ℓ are the uniform dyadic abscissas, with multiple nodes at the segment end points,

$$(\xi_i^\ell)_{i\in\mathbb{Z}} = (\ldots, 0, 0, 0, \tfrac{1}{2^\ell}, \tfrac{2}{2^\ell}, \tfrac{3}{2^\ell}, \ldots, \tfrac{2^{\ell+1}-1}{2^\ell}, 1, 1, 1, \ldots) \,.$$

It is evident that this selection does not ensure the strict monotonicity that is presumed to be satisfied by the nodes. However, we are using it here to explain the decay phenomenon.

The initial set T^0_{PHT} of PHT-splines contains the 6 cubic B-splines defined by the knot vector $(0, 0, 0, 0, 1, 1, 2, 2, 2, 2)$, which are shown in Fig. 3(a). After truncating and enriching once and twice, we obtain the sets T^1_{PHT} and T^2_{PHT}, which are shown in Figs. 3(b) and (c), respectively. While the truncation works well for most of the PHT-splines, the second and the penultimate PHT-spline basis functions decay quickly as the level increases. In each step, the maximum value attained by them shrinks approximately by 50%. Clearly this extends to bivariate PHT-splines, which is obvious when considering the domain $\Omega^0 = (0, 2)^2$ and refining it uniformly.

Zhu and Chen [36] addressed this "decay phenomenon" by modifying the original construction of PHT-splines, as follows:

Step 1. The first step is the same as for constructing PHT-splines, which has been described in Section 4.

Step 2. Second, we iteratively *truncate, modify and enrich* these sets of B-systems. We begin by initializing the construction with the B-systems selected at the coarsest level. Then, we iteratively truncate the functions with respect to the selected B-systems of the next level. Truncated B-systems with rectangular (i.e., box-shaped) supports are *modified* by replacing them with standard (i.e., non-truncated) B-systems. Simultaneously, we enrich the basis by adding the selected B-systems of the next level. More precisely, we define

$$M^\ell_{\mathrm{PHT}} = \mathrm{trc\&mod}^\ell_{\mathrm{PHT}}\, M^{\ell-1}_{\mathrm{PHT}} \cup S^\ell$$

This gives $M^0_{\mathrm{PHT}} = S^0_{\mathrm{PHT}}$ since we define $M^{-1}_{\mathrm{PHT}} = \emptyset$. The resulting truncated, modified and enriched sets of B-systems

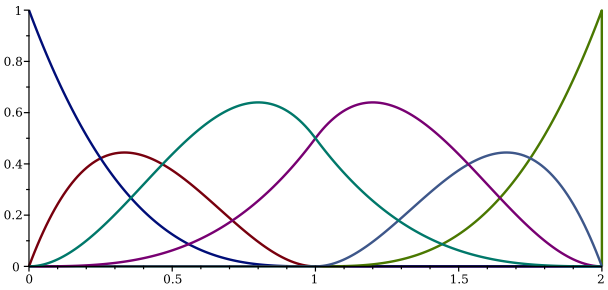

(a) The set T^0_{PHT}

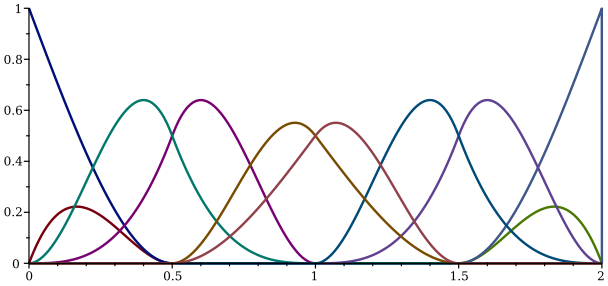

(b) The set T^1_{PHT}

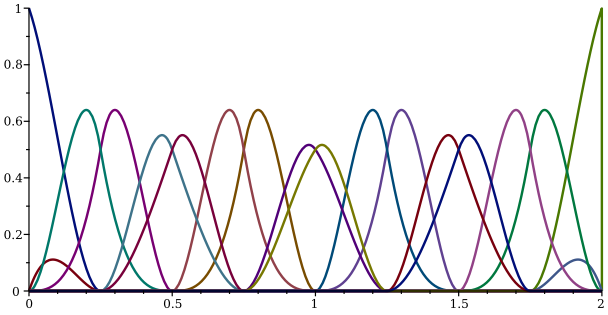

(c) The set T^2_{PHT}

Fig. 3 Univariate PHT-splines on a uniformly refined interval. The second and the last but one PHT-spline experience the "decay phenomenon".

$$M^{\ell}_{\mathrm{PHT}} = \bigcup_{k=0}^{\ell} \{B^{k,\ell}_{i,j} \mid (i,j) \in \mathcal{I}^{\ell}_{\mathrm{PHT}}\}$$

are formed by sets of selected B-systems of levels $k = 0, \ldots, \ell$, which have been truncated and modified $\ell - k$ times, i.e.,

$$B^{k,\ell}_{i,j} = \begin{cases} \mathrm{trc\&mod}^{\ell}_{\mathrm{PHT}}\, B^{k,\ell-1}_{i,j} & \text{if } k < \ell\,, \\ B^{\ell}_{i,j} & \text{if } k = \ell\,. \end{cases}$$

In addition to the previously described truncation, we modify each truncated B-system by replacing it with a standard (i.e., non-truncated) B-system if it has box support, i.e.,

$$\text{trc\&mod}^{\ell}_{\text{PHT}}\, B^{k,\ell-1}_{i,j} = \begin{cases} B_{(\xi',\xi''),(\eta',\eta'')} \\ \qquad \text{if } \operatorname{supp}(\text{trc}^{\ell}_{\text{PHT}}\, B^{k,\ell-1}_{i,j}) = (\xi',\xi'') \times (\eta',\eta'') \,, \\ \text{trc}^{\ell}_{\text{PHT}}\, B^{k,\ell-1}_{i,j} \\ \qquad \text{if } \operatorname{supp}(\text{trc}^{\ell}_{\text{PHT}}\, B^{k,\ell-1}_{i,j}) \text{ is not a box.} \end{cases}$$

Each M^{ℓ}_{PHT} for $\ell = 0, \ldots, L$ is a set of sets of B-splines.

Step 3. Finally we define the modified basis $\mathbb{B}_{\text{MPHT}} = \bigcup M^{L}_{\text{PHT}}$.

Once more, the construction of the MPHT-splines ensures the following property, the proof of which is analogous to that of the PHT-spline basis:

Corollary 7 *Only MPHT-splines originating from exactly one of the B-systems (and subsequently truncated and modified) take non-zero values and derivatives considered in* (1) *at each cross vertex and at each boundary vertex.*

As with PHT- and THB-splines, the MPHT-splines form a *non-negative partition of unity* as a consequence of this fact.

The modification does not change the support of the B-systems, hence we have the following result:

Proposition 8 *The supports of the PHT- and MPHT-splines associated with the same cross or boundary vertex of the hierarchical mesh are identical.*

We refer again to Figure 1, which depicts the B-systems formed by the PHT- and MPHT-splines for a specific two-level hierarchical grid.

7 New PHT-splines

A new basis of the spline space $\mathcal{S}$ was introduced by Kang et al. [12]. It is generated by the construction described below:

Step 1. The first step is the same as for constructing PHT-splines, which has been described in Section 4.

Step 2. Second, we iteratively *truncate, modify and enrich* these sets of B-systems. This step is the same as for constructing the Modified PHT-splines, which has been described in Section 6.

Step 3. Finally we *tensorize* all the resulting B-systems. Recall that the set M^{L}_{PHT} consists of selected B-systems $B^{k,L}_{i,j}$, with indices $(i,j) \in \mathcal{I}^{k}_{\text{PHT}}$ and levels $k = 0, \ldots, L$, which have been truncated and modified $L-k$ times. We tensorize them

by replacing them with B-systems that are defined on the axis-aligned bounding box (denoted as bb(.)) of their support,

$$\begin{aligned}\text{tens } B_{i,j}^{k,L} &= B_{(\xi',\xi_i^k,\xi''),(\eta',\eta_j^k,\eta'')} \\ &\qquad \text{if bb}(\text{supp}(B_{i,j}^{k,L})) = (\xi',\xi'') \times (\eta',\eta'') \ .\end{aligned}$$

In other words, the additional nodes of these B-systems are chosen as

$$\begin{aligned}\xi' &= \inf\{x \mid \exists y : (x,y) \in \text{supp}(B_{i,j}^{k,L})\} \ , \\ \xi'' &= \sup\{x \mid \exists y : (x,y) \in \text{supp}(B_{i,j}^{k,L})\} \ , \\ \eta' &= \inf\{y \mid \exists x : (x,y) \in \text{supp}(B_{i,j}^{k,L})\} \ , \\ \eta'' &= \sup\{y \mid \exists x : (x,y) \in \text{supp}(B_{i,j}^{k,L})\} \ .\end{aligned}$$

Note that only B-systems with non-rectangular supports are actually replaced, since the remaining ones already possess this form as a result of the modification step in the construction of MPHT-splines.

The resulting truncated, modified, enriched and tensorized sets of B-systems

$$M_{\text{NPHT}} = \bigcup_{k=0}^{L} \{\text{tens } B_{i,j}^{k,L} \mid (i,j) \in \mathcal{I}_{\text{PHT}}^k\}$$

are formed by sets of selected B-systems of levels $k = 0, \ldots, L$, which have been truncated and modified $L - k$ times, and were finally tensorized. Again, M_{NPHT} is a set of sets of B-splines.

Step 4. Finally we define the new basis $\mathbb{B}_{\text{NPHT}} = \bigcup M_{\text{NPHT}}$.

As a major difference to the other bases, NPHT-splines originating from *more than one of the B-systems* (and subsequently truncated, modified and tensorized) may take non-zero values and derivatives considered in (1) at each cross vertex and at each boundary vertex. Consequently, the MPHT-splines do not necessarily form a *partition of unity*. The non-negativity property is, however, trivially satisfied.

Nevertheless, NPHT-splines inherit the ordering of their associated vertices, similar to HB-splines, and are therefore linearly independent, see [12] for details.

Figure 4 depicts the B-systems formed by the NPHT-splines (see Section 6) for a specific two-level hierarchical grid.

We conclude this section by noting a connection to the locally refined (LR) B-splines of Dokken et al. [5]. Recall that each B-system (2) is associated with the 3×3 *local grid*

$$\big(\{\xi', \xi'', \xi'''\} \times [\eta', \eta'''] \big) \cup \big([\xi', \xi'''] \times \{\eta', \eta'', \eta'''\}\big)$$

of knot lines. A B-system is said to be *on the grid* if its local grid is a subset of the hierarchical grid $\mathcal{G}$. (To streamline the presentation, we do not discuss boundary cells; they can be handled,e.g., by introducing a phantom boundary layer.) A B-

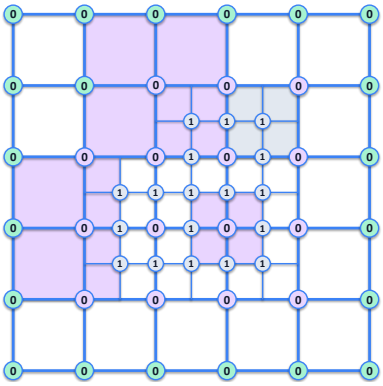

Fig. 4 B-systems formed by NPHT-splines on a two-level hierarchical grid. All truncated level-0 MPHT-systems (cf. Fig. 1) are modified into standard B-systems (purple).

system that is on the grid is said to be *reachable* if its local grid is a subset of a grid obtained by adding a single vertical or horizontal line to the local grid of another reachable B-system; the former is then said to be a *descendant* of the latter one. All the B-systems on the coarsest rectangular grid Γ^0 are declared reachable, which initializes the set of reachable B-systems. Finally, the *LR B-splines on* $\mathcal{G}$ are the elements of the *reachable* B-systems *with no descendants* that take non-zero values on Ω^0. These are closely related to the NPHT-splines of Kang et al. [12]:

Theorem 9 *The NPHT-splines are LR B-splines if none of the edge–connected*[1] *components of each subdomain* Ω^ℓ *for* $\ell = 1, \ldots, N$ *is a single cell of level* $\ell - 1$.

Proof First we prove that a B-system $B^\ell_{i,j}$ is reachable whenever $(\xi^\ell_i, \eta^\ell_j)$ is a level-ℓ vertex that belongs to a subdomain Ω^ℓ for any $\ell = 0, \ldots, L$. For the coarsest level ($\ell = 0$) this is implied directly by the definition of reachability.

To extend the result to higher levels, we proceed by induction from ℓ to ℓ+1. Under our refinement rule (which forbids refining a single cell in isolation), any level-(ℓ+1) vertex is one of the three inner vertices created by refining an edge-connected pair of two level-ℓ cells in $\Omega^{\ell+1}$ by cross insertion. Moreover, this pair necessarily belongs to a compound of 2×2 level-ℓ cells in Ω^ℓ.

By the induction hypothesis, the central level-ℓ vertex of the latter compound has an associated reachable level-ℓ B-system. By adding the level-(ℓ+1) edges in the order shown in Fig. 5a, we then demonstrate the reachability of the three level-(ℓ+1) B-systems associated with the three inner cross vertices of the pair of level-ℓ cells. The three types of hatching indicate the supports of these three B-systems (upwards diagonally, vertically, and downwards diagonally).

[1] Two level-ℓ cells that share an edge are said to be edge-adjacent; the edge-connected components of Ω^ℓ are the maximal sets of cells in which any two cells can be linked by a finite chain of edge-adjacent cells (i.e., by the transitive closure of this relation).

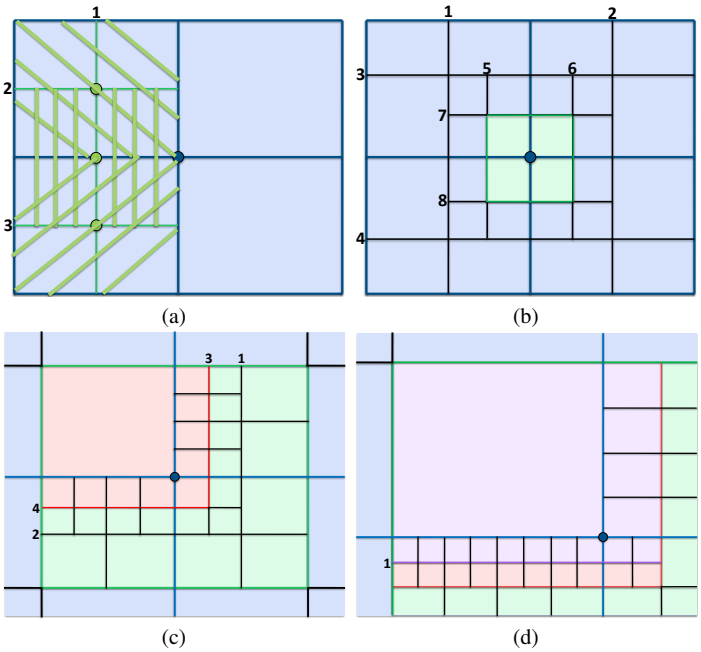

Fig. 5 (a) Proving the reachability of B-systems associated with level-$(\ell+1)$ vertices in the subdomain $\Omega^{\ell+1}$. (b-d) The structure of the axis-aligned bounding box of the support of a THB-spline.

Second we consider the B-system of THB-splines associated with a vertex $(\xi_i^\ell, \eta_j^\ell)$ of level ℓ. We demonstrate that the axis-aligned bounding box of its support necessarily has the structure shown in Fig. 5d (the light purple-shaded rectangle), up to isometries and homeomorphisms of the two coordinate axes[2]. This structure is governed by three levels $\ell' \le \ell'' \le \ell'''$, where $\ell' \ge \ell$, which determine the axis-aligned bounding box of the support.

Indeed, if we consider the right boundary of the box, which is determined by a knot, say, $\xi_{\hat{\imath}}^{\hat{\ell}}$, of level $\hat{\ell}$, then that knot comes immediately after $\xi_i^\ell = \xi_{2^{\hat{\ell}-\ell}i}^{\hat{\ell}}$ in the level-$\hat{\ell}$ knot sequence, i.e., $\hat{\imath} = 2^{\hat{\ell}-\ell}i + 1$. Assuming otherwise would result in a vertical line determined by a lower-level knot between the two, which contradicts the assumption. Analogous arguments can be used for the remaining three boundaries. Also, two of the four boundaries must possess the same level and be adjacent to each other.

Figs. 5b-d depict the construction of the axis-aligned bounding box (recall that it is shown as the light purple-shaded rectangle in Fig. 5d). First, the level increases from ℓ to ℓ' in Figs. 5a, creating (e.g.) the northern and western boundaries. Second, the level increases from ℓ' to ℓ'' in Fig. 5b, creating (e.g.) the eastern boundary.

[2] These homeomorphisms are applied to each coordinate axis individually and are necessary for allowing non-uniform knot sequences.

Finally, the level increases from ℓ'' to ℓ''' in Fig. 5b, creating (e.g.) the southern boundary. Each figure c,d zooms into a portion of the preceding one. We chose $\ell''' = \ell'' + 1 = \ell' + 3 = \ell + 5$ for the visualization. Additional refinements that do not affect the bounding box may be present.

We then use this fact to demonstrate the reachability of the B-system associated with the grid that defines the axis-aligned bounding box. This is done by adding the edges in the order shown in Fig. 5b-d. Clearly, this B-system has no descendants since it is defined by the axis-aligned bounding box of the THB-spline in the B-system.

Finally we complete the proof by noting that the supports of THB- and MPHT-splines–and hence their axis-aligned bounding boxes–are the same, cf. Propositions 6 and 8. □

This assumption is necessary, as can be seen by considering a mesh of level 0 that is refined by splitting exactly one cell into four smaller ones. The LR B-splines do not generate additional basis functions, unlike the NPHT-splines.

Securing linear independence of general LR B-splines is a long-standing open problem. According to the above Theorem, the basis property of NPHT-splines (noted by Kang et al. [12]) establishes linear independence for a particular class of LR B-splines.

8 Comparison

The PHT, THB and MPHT-splines, despite having the same supports of the basis functions, are generally different if $r \geq 1$.

- For a vertex of level ℓ that is contained within higher-level subdomains, the PHT-spline construction uses truncation to generate basis functions from B-systems of level ℓ. The THB-splines, on the other hand, use higher level B-systems in their construction. Consequently, different functions are created for vertices contained within higher-level subdomains.
- The construction of MPHT-splines generates B-systems (i.e., products of univariate B-splines) whenever the support is box-shaped. The THB-splines, on the other hand, are generated via truncation for all level ℓ vertices along the boundary of the subdomain $\Omega^{\ell+1}$. Even if the resulting support is box shaped, the truncation does not generate a B-system. Instead, it generates a linear combination thereof.

Table 2 summarizes the properties of the various bases. In addition to the constructions described in this paper, it also includes the Hermite basis (known as Bogner-Fox-Schmit (BFS) elements on rectangles with hanging nodes in the finite element literature [15]).

In addition to the previously described properties, the table includes a result concerning the local linear independence property. Recall that a system of functions has this property if the functions that take non-zero values on any subdomain are

linearly independent when restricted to that subdomain. We need to assume mesh grading, i.e., the level difference between adjacent cells does not exceed one[3].

Theorem 10 *The BFS-, PHT-, THB- and MPHT-splines possess the property of local linear independence if we assume mesh grading.*

Proof We construct the hierarchical T-mesh by successive cross insertions, proceeding from the coarsest to the finest level. Specifically, for each level $\ell = 0, \ldots, L-1$, we refine every level-ℓ cell that has been selected for refinement, i.e., each cell contained in $\Omega^{\ell+1}$.

First, we show by induction that, up to isometries and homeomorphisms of the two coordinate axes[4], every interior cell belongs to one of the nine types depicted in Fig. 6. To streamline the presentation, we do not discuss boundary cells; they can be handled either by enlarging the catalog of types or by introducing a phantom boundary layer.

The base case is the initial mesh, in which all cells are of type A1. For the inductive step, observe that a cross insertion (applied wherever allowed by the mesh-grading constraints) transforms any catalogued cell into a configuration of four cells, each again of one of the eight types. Furthermore, when a neighboring cell undergoes cross insertion (again subject to mesh grading), the type of the original cell may change, but it remains within the same catalog. The resulting type transitions are summarized in Table 1.

cell	cross insertion:				neighboring cell refinement:			
type	top left	top right	bottom left	bottom right	eastern	northern	western	southern
A1	C	C	C	C	A2	A2	A2	A2
A2	B1	B1	C	C	A3	–	A3	A4
A3	A1	B1	B1	C	A5	–	–	A5
A4	B1	B1	B1	B1	A5	–	A5	–
A5	A1	B1	A1	B1	A6	–	–	–
A6	A1	A1	A1	A1	–	–	–	–
B1	×	×	×	×	×	A1	×	B2
B2	×	×	×	×	×	A2	×	–
C	×	×	×	×	×	B1	B1	×

Table 1 List of type transitions. Refining a cell through cross insertion creates four cells of the four types listed in columns 2-5. Refining a neighboring cell by cross insertion transforms the cell into the type listed in columns 6-9. Certain cross insertions (marked by − and ×) are not possible because the cell has already been refined (−), or because doing so would violate the mesh grading assumption (×).

Second, we prove the theorem for THB-splines. Under the mesh-grading assumption, B-systems from at most two levels are active on any cell of the hierarchical mesh. Indeed, each subdomain Ω^{ℓ} has a boundary layer of level-ℓ cells, and the support of the selected THB-systems from the previous level (i.e., $\ell - 1$) does not extend

[3] Here, we consider the standard definition of adjacency, whereby cells that share segments of edges or vertices are declared adjacent.

[4] Cf. Footnote 2

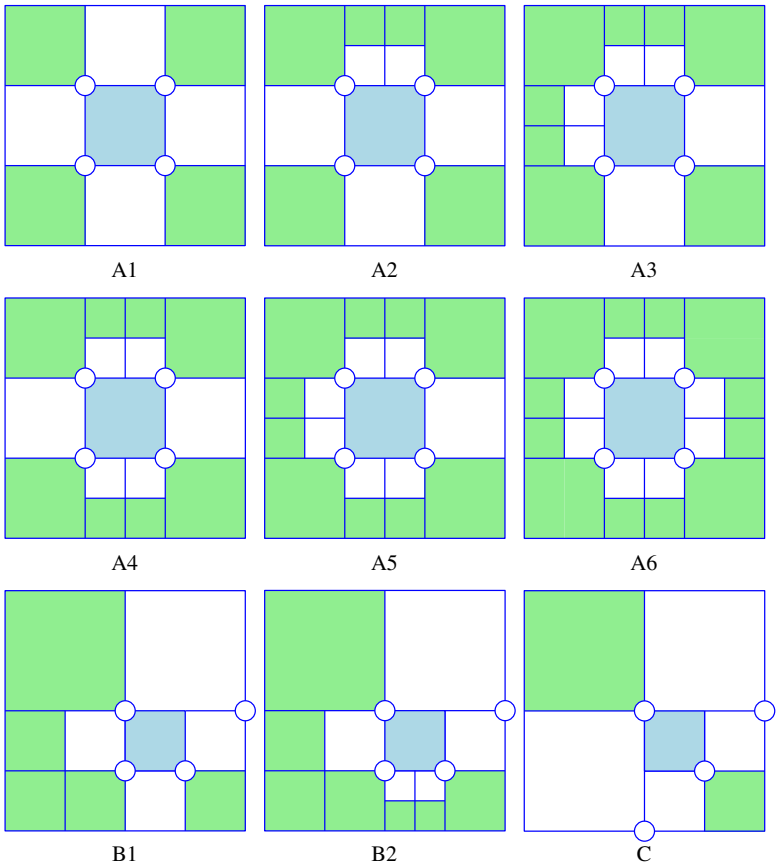

Fig. 6 Catalog of cell types in hierarchical T-meshes with mesh grading. Further refinement may be present within the green-shaded regions.

beyond this layer. Consequently, the B-systems active on a given cell are precisely those associated with certain cross vertices that are visible in the local configuration of each of the nine cell types. A case-by-case inspection confirms that, for every cell type, the active B-systems are exactly those corresponding to the four cross vertices marked by circles. This establishes the local linear independence of the B-systems formed by THB-splines.

Finally, we extend the result to the other three types of B-systems. For each cross vertex, the functions that comprise these types of B-systems can be obtained by linearly combining the THB-splines of the B-system since the support of the functions is identical and does not include any other cross vertex. The proof is complete. □

For the sake of completeness, Figure 7 shows an example of local linear independence being violated when no mesh grading assumption is made.

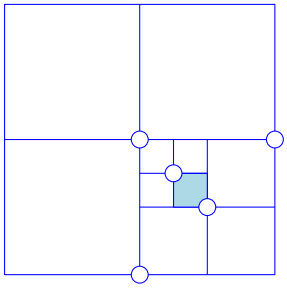

Fig. 7 A hierarchical mesh without local linear independence: Five B-systems are active in the marked cell.

Finally we rank the basis according to the size of the supports of the basis functions. PHT, THB, and MPHT have the smallest supports, HB has the largest supports, and NPHT is in between. In addition we rank the basis according to the percentage of the tensor-product B-splines which are present in the basis (advantageous for implementation and assembly). The maximum number is realized by NPHT and HB (both 100%), with MPHT being the second best option.

		BFS	PHT	HB	THB	MPHT	NPHT
Properties:	Linear independence	✓	✓	✓	✓	✓	✓
	Local linear independence	✓	✓	✗	✓	✓	✗
	Algebraic completeness	✓	✓	✓	✓	✓	✓
	Non-negativity	✗	✓	✓	✓	✓	✓
	Partition of unity	✗	✓	✗	✓	✓	✗
Rankings:	Small size of the supports	1.	1.	3.	1.	1.	2.
	Presence of tensor-product B-splines	5.	4.	1.	3.	2.	1.

Table 2 Properties and rankings of bases for splines on hierarchical T-meshes.

9 Conclusions and future work

This paper has provided a systematic comparison of hierarchical spline constructions, including PHT-splines, HB-splines and THB-splines, modified PHT-splines and new PHT-splines. Our analysis demonstrates that each construction presents unique trade-offs between fundamental properties.

Among all options, modified PHT-splines (MPHT-splines) emerge as the optimal choice. They preserve all the essential properties of PHT-splines and THB-splines including linear independence, local linear independence, completeness,

non-negativity, and partition of unity, while containing a higher proportion of tensor-product B-splines than THB-splines. This makes MPHT-splines particularly advantageous for isogeometric analysis, as the preserved tensor-product structure significantly enhances computational efficiency in evaluation and matrix assembly.

A key direction for future work is to extend these constructions, particularly NPHT-splines (which we have identified as a subclass of LR B-splines), to support anisotropic local refinement while preserving local linear independence. This property is essential for building efficient spline projectors and yields favorable sparsity in the resulting numerical discretizations. Several refinement strategies that ensure local linear independence have been proposed in the literature [1, 9, 10, 25, 26, 28]. While the relevant phenomena are by now fairly well understood for bivariate C^r-smooth splines of degree $2r + 1$, the extension to higher dimensions and lower degrees warrants further investigation.

References

1. A. Bressan and B. Jüttler. A hierarchical construction of LR meshes in 2D. *Computer Aided Geometric Design*, 37:9–24, 2015.
2. C. L. Chan, C. Anitescu, and T. Rabczuk. Volumetric parametrization from a level set boundary representation with PHT-splines. *Computer-Aided Design*, 82:29–41, 2017.
3. J. Deng, F. Chen, and Y. Feng. Dimensions of spline spaces over T-meshes. *Journal of Computational and Applied Mathematics*, 194(2):267–283, 2006.
4. J. Deng, F. Chen, X. Li, C. Hu, W. Tong, Z. Yang, and Y. Feng. Polynomial splines over hierarchical T-meshes. *Graphical Models*, 70(4):76–86, 2008.
5. T. Dokken, T. Lyche, and K. F. Pettersen. Polynomial splines over locally refined box-partitions. *Computer Aided Geometric Design*, 30(3):331–356, 2013.
6. A. Falini, J. Špeh, and B. Jüttler. Planar domain parameterization with THB-splines. *Computer Aided Geometric Design*, 35:95–108, 2015.
7. C. Giannelli, B. Jüttler, S. K. Kleiss, A. Mantzaflaris, B. Simeon, and J. Špeh. THB-splines: An effective mathematical technology for adaptive refinement in geometric design and isogeometric analysis. *Computer Methods in Applied Mechanics and Engineering*, 299:337–365, 2016.
8. C. Giannelli, B. Jüttler, and H. Speleers. THB-splines: The truncated basis for hierarchical splines. *Computer Aided Geometric Design*, 29(7):485–498, 2012.
9. L. Groiss, B. Jüttler, and M. Pan. Local linear independence of bilinear (and higher degree) B-splines on hierarchical T-meshes. *Computer Aided Geometric Design*, 103:102190, 2023.
10. L. Groiss, B. Jüttler, and M. Pan. On tensor-product bases of PHT-spline spaces. In M. Lanini, C. Manni, and H. Schenck, editors, *Approximation Theory and Numerical Analysis Meet Algebra, Geometry, Topology*, volume 60 of *INdAM series*, pages 181–203, Singapore, 2024. Springer.
11. A. Gupta, B. Mamindlapelly, P. L. Karuthedath, R. Chowdhury, and A. Chakrabarti. Adaptive isogeometric topology optimization using PHT splines. *Computer Methods in Applied Mechanics and Engineering*, 395:114993, 2022.
12. H. Kang, J. Xu, F. Chen, and J. Deng. A new basis for PHT-splines. *Graphical Models*, 82:149–159, 2015.
13. G. Kermarrec, V. Skytt, and T. Dokken. Adaptive Surface Fitting with Local Refinement: LR B-Spline Surfaces. In *Optimal Surface Fitting of Point Clouds Using Local Refinement: Application to GIS Data*, pages 23–39. Springer, 2022.

14. G. Kiss, C. Giannelli, U. Zore, B. Jüttler, D. Großmann, and J. Barner. Adaptive CAD model (re-) construction with THB-splines. *Graphical Models*, 76(5):273–288, 2014.
15. S. Kleiss, B. Jüttler, and W. Zulehner. Enhancing isogeometric analysis by a finite element-based local refinement strategy. *Computer Methods in Applied Mechanics and Engineering*, 213-216:168–182, 2012.
16. R. Kraft. *Adaptive und linear unabhängige Multilevel B-Splines und ihre Anwendungen*. PhD thesis, Universität Stuttgart, 1998.
17. X. Li, J. Zheng, T. W. Sederberg, T. J. Hughes, and M. A. Scott. On linear independence of T-spline blending functions. *Computer Aided Geometric Design*, 29(1):63–76, 2012.
18. S. Merchel, B. Jüttler, D. Mokriš, and M. Pan. Fast formation of matrices for least-squares fitting by tensor-product spline surfaces. *Computer-Aided Design*, 150:103307, 2022.
19. D. Mokriš, B. Jüttler, and C. Giannelli. On the completeness of hierarchical tensor-product B-splines. *Journal of Computational and Applied Mathematics*, 271:53–70, 2014.
20. L. Noël, M. Schmidt, C. Messe, J. Evans, and K. Maute. Adaptive level set topology optimization using hierarchical B-splines. *Structural and Multidisciplinary Optimization*, 62(4):1669–1699, 2020.
21. M. Pan and F. Chen. Constructing planar domain parameterization with HB-splines via quasi-conformal mapping. *Computer Aided Geometric Design*, 97:102133, 2022.
22. M. Pan, B. Jüttler, and A. Giust. Fast formation of isogeometric Galerkin matrices via integration by interpolation and look-up. *Computer Methods in Applied Mechanics and Engineering*, 366:113005, 2020.
23. M. Pan, B. Jüttler, and A. Mantzaflaris. Efficient matrix assembly in isogeometric analysis with hierarchical B-splines. *Journal of Computational and Applied Mathematics*, 390:113278, 2021.
24. M. Pan, B. Jüttler, and F. Scholz. Efficient matrix computation for isogeometric discretizations with hierarchical B-splines in any dimension. *Computer Methods in Applied Mechanics and Engineering*, 388, 2022.
25. M. Pan, R. Zou, and B. Jüttler. Algorithms and data structures for C^s-smooth RMB-splines of degree $2s + 1$. *Computer Aided Geometric Design*, 114:102389, 2024.
26. F. Patrizi. Effective grading refinement for locally linearly independent LR B-splines. *BIT Numerical Mathematics*, 62(4):1745–1764, 2022.
27. F. Patrizi and T. Dokken. Linear dependence of bivariate Minimal Support and Locally Refined B-splines over LR-meshes. *Computer Aided Geometric Design*, 77:101803, 2020.
28. F. Patrizi, C. Manni, F. Pelosi, and H. Speleers. Adaptive refinement with locally linearly independent LR B-splines: Theory and applications. *Computer Methods in Applied Mechanics and Engineering*, 369:113230, 2020.
29. T. W. Sederberg, J. Zheng, A. Bakenov, and A. Nasri. T-splines and T-NURCCs. *ACM Transactions on Graphics*, 22(3):477–484, 2003.
30. K. Shepherd and D. Toshniwal. Locally-verifiable sufficient conditions for exactness of the hierarchical B-spline discrete de Rham complex in $\mathbb{R}^n$. *Foundations of Computational Mathematics*, pages 1–43, 2024.
31. H. Speleers and C. Manni. Effortless quasi-interpolation in hierarchical spaces. *Numerische Mathematik*, 132:155–184, 2016.
32. P. Wang, J. Xu, J. Deng, and F. Chen. Adaptive isogeometric analysis using rational PHT-splines. *Computer-Aided Design*, 43(11):1438–1448, 2011.
33. X. Xie, S. Wang, Y. Wang, N. Jiang, W. Zhao, and M. Xu. Truncated hierarchical B-spline–based topology optimization. *Structural and Multidisciplinary Optimization*, 62(1):83–105, 2020.
34. X. Zhang, M. Xiao, W. Luo, L. Gao, and J. Gao. Isogeometric topology optimization for innovative designs of the reinforced TPMS unit cells with curvy stiffeners using T-splines. *Composite Structures*, 357:118955, 2025.
35. Y. Zhang, W. Wang, and T. J. Hughes. Solid T-spline construction from boundary representations for genus-zero geometry. *Computer Methods in Applied Mechanics and Engineering*, 249:185–197, 2012.
36. Y. Zhu and F. Chen. Modified bases of PHT-splines. *Communications in Mathematics and Statistics*, 5(4):381–397, 2017.